A New Model Predictive Control Method for Eliminating Hydraulic Oscillation and Dynamic Hydraulic Imbalance in a Complex Chilled Water System

Yang Yuan [1,2], Neng Zhu [1], Haizhu Zhou [2] and Hai Wang [2,*]

[1] School of Environmental Science and Engineering, Tianjin University, Tianjin 300350, China; 13810969897@163.com (Y.Y.); nzhu@tju.edu.cn (N.Z.)
[2] China Academy of Building Research, Beijing 100013, China; zhznhm@163.com
[*] Correspondence: tjneowanghai@163.com

Abstract: To enhance the energy performance of a central air-conditioning system, an effective control method for the chilled water system is always essential. However, it is a real challenge to distribute exact cooling energy to multiple terminal units in different floors via a complex chilled water network. To mitigate hydraulic imbalance in a complex chilled water system, many throttle valves and variable-speed pumps are installed, which are usually regulated by PID-based controllers. Due to the severe hydraulic coupling among the valves and pumps, the hydraulic oscillation phenomena often occur while using those feedback-based controllers. Based on a data-calibrated water distribution model which can accurately predict the hydraulic behaviors of a chilled water system, a new Model Predictive Control (MPC) method is proposed in this study. The proposed method is validated by a real-life chilled water system in a 22-floor hotel. By the proposed method, the valves and pumps can be regulated safely without any hydraulic oscillations. Simultaneously, the hydraulic imbalance among different floors is also eliminated, which can save 23.3% electricity consumption of the pumps.

Keywords: chilled water system; model predictive control; hydraulic oscillation; pipe network; high-rise building

1. Introduction

The energy consumptions in the buildings sector account for almost 40% of the total final energy consumption [1,2]. Previous studies showed that heating, ventilation, and air conditioning (HVAC) systems take up almost 50% of energy use in buildings [3]. To enhance energy savings in HVAC systems, many solutions have been applied in the last few decades. Obviously, the control methods are effective approaches with minimal additional cost. With the decreased costs of Data Collecting System (DCS), Cloud Service (CS), and Remote Control (RC), etc. in recent years, the design and implementation of more complex control techniques have become feasible [4–6].

Classical on/off and PID control methods are still widely used in many HVAC systems due to simplicity and lower investment, causing inconsistent performance among these systems. With the help of the modern automation and information technologies, many advanced control methods can be adopted to improve the safety and efficiency of the HVAC systems. Model Predictive Control (MPC) is one of the promising control approaches for future low energy building. Research on the MPC method has attracted a lot of attention in the past few years due to its many advantages, such as: performing anticipatory control instead of corrective control [7] and ability to deal with constraints and uncertainties [8]. Recently, Abdul and Farrokh [9] presented a comprehensive literature review of control methods with an emphasis on the theory and applications of MPC for HVAC systems. Recently, Abdul and Farrokh [9] presented a comprehensive literature review of control methods, focusing on the theory and applications of MPC for HVAC systems. Compared with the PID, Robust and Fuzzy control methods, MPC control strategies

have special advantages for nonlinear and time-varying dynamics of the holistic or part of an HVAC system.

Generally, an MPC method depends on a system model to predict the future behavior of the object system, generating a control vector that minimizes a certain object function within the prediction horizon with the existence of disturbances and constraints. With respect to the factors affecting MPC performance, the system models are of vital importance. For most pragmatic MPC methods, their system models are mainly from two aspects: physics-based model or data-based model [10]. The physics-based models, or white box models, are based on the principles of the thermal dynamics and hydraulic dynamics. The parameters of the pumps, coils and chillers, etc. are determined from manufacturer documentation or estimation techniques on measured data. Many physics-based models for HVAC components and systems have been developed in literature. Tashtoush et al. [11] proposed a procedure for obtaining a dynamic model of an HVAC system, which is comprised of a zone, heating coil, cooling coil, dehumidifying coil, humidifier, fan, ductwork, and mixing box. Kohlenbach et al. [12] presented a dynamic model for single-effect LiBr/water absorption chillers. Chen et al. [13] introduced a simulation platform with a customized Simulink block library for a dynamic HVAC component model, including a conduit, damper/valve, fan/pump, flow merge, flow split, cooling and heating coil, and zone. Jin et al. [14] developed a dynamic cooling coil unit model using the mass and energy balance equations. These physics-based models have been extensively used in some MPC approaches, such as the zone temperature process [15], mixed-mode cooling [16], floor heating system [17] and ice storage involved cooling system [18]. There are already some HVAC simulation tools available for comprehensive modeling, such as Energy Plus [19], TRNSYS [20], and Simulink [21]. These software tools are usually employed to evaluate the performance of a controller rather than the development of a real one. Many assumptions and simplification have to be made to reduce computational burden for a practical MPC controller. The hydraulic balance of the chilled water system was rarely considered in physical models. However, the hydraulic balance has significant influence on the energy performance of a complex chilled water system [22]. Furthermore, the hydraulic oscillations often take place while applying a conventional PID-based control system, which may cause the water hammer which damages the water pipe network. A sophisticated design of the MPC-based control system should consider how to eliminate the hydraulic oscillation and dynamic hydraulic imbalance simultaneously. This aspect would be the emphasis of this paper.

As regards the data-based models or black-box models, they are developed via measured data. These models use mathematical methods (such as statistical regression or artificial neural networks) to establish the relationship between input and output variables. The data-based models can be developed without too much understanding of system physics. Abdul et al. [23] presented a comprehensive review on the artificial neural network (ANN) based MPC system design and case studies. Fabrizio et al. [24] proposed a new MPC approach using a Genetic Algorithm (GA) to support cost-optimal design of building and HVAC systems. In recent years, researchers have proposed many types of data-based models, such as frequency domain models [25], data mining algorithms [26,27], fuzzy logic models [28,29], and statistical models [30,31]. However, the accuracy of a data-based model highly depends on the training data covering all the operating conditions, which could be a challenge for complex HVAC systems. Most data-based MPC methods are applied at the supervisory level to optimize the energy use, cost, and thermal comfort at the building scale. Then, the MPC platform at supervisory level still depend on a PID-based controller at the local level to adjust valves and pumps to designated set points. Therefore, the hydraulic oscillation phenomena still cannot be eliminated. New MPC-based controllers at the local level are urgently required to work consistently with the supervisory MPC platform.

As regards the chilled water system, Ma and Wang presented a fruitful work on control approaches for complex central chilled water systems [32,33]. Shan et al. [34] proposed an MPC method to control the charging/discharging of thermal energy storage and on/off

chillers to achieve high efficiency. Recently, Gianni et al. [35] proposed a specialized MPC approach to control the HVAC system and the storage devices under thermal comfort and technological limitations.

In this paper, the contributions are mainly in two aspects: (1) A new MPC method is proposed to achieve the dynamic hydraulic balance for the chilled water distribution system. In this procedure, a system model is developed with considering the hydraulic characteristics of the chillers, terminal units, throttle valves, pumps and pipe network in detail. An optimization model using a GA algorithm is also presented to provide the calibrated parameters for the system model; (2) two types of MPC-based controllers at the local level are elaborately designed for adjustments of throttle valve and variable-speed pump, respectively. Instead of those PID-based controllers, the local MPC-based controllers can work more smoothly with the supervisory MPC platform. In addition, to validate the proposed MPC method, a round of regulation is demonstrated step by step in a real-life case study. With the help of the automation system and information technologies, the dynamic hydraulic balance was achieved without any hydraulic oscillations in the tested chilled water system.

2. System Description and Two Control Mechanism

For a complex chilled water system, how to distribute the exact cooling energy to multiple terminal units depends on accurate load prediction and an effective control method. There are already many previous studies dedicated to air-conditioning load prediction [36,37]. In this paper, we focus on the safety and efficiency of the new control method.

2.1. Chilled Water Distribution System

A typical chilled water distribution system is composed of chillers, terminal units (such as AHU or Coil), pumps, valves and numerous pipes, etc. A diagram of a typical configuration of chilled water distribution system in a high-rise building is shown in Figure 1.

The chillers provide cooling energy to circulating water. There are also heat rejection units for the chillers, which are not shown in Figure 1. The primary pumps that serve those chillers usually operate at a constant speed. The supplementary pump and water tank are used to provide a stable pressure head for the inlet of the primary pumps. At the outlet of the chillers, a common leg is employed to guarantee the chillers with enough and stable water flow. The secondary pumps are often operated at variable speed according to the cooling demands. The throttle valves are installed at the entrance of each floor, which are adjusted by the controllers to achieve a hydraulic balance between different floors. There are also many on/off valves installed at the entrance of the terminal units, which can be controlled by a local user or an upper supervisory controller.

2.2. Feedback Control Method

In a conventional control method, the valves are usually tuned by PID-based controllers. A schematic control diagram of typical PID control method is shown in Figure 2.

In a typical PID-based control method, the openness of the valves and rotation speed of the pumps are adjusted by those PID controllers. The set point for a controller is vitally important. The set-points come from the upper supervisory platform or onsite user. Usually, one or several indoor temperature sensors can be employed to provide the current indoor temperature (T_{indoor}). The temperature errors between current points and set points are used as feedback signals for the controllers to adjust valves. The return water temperature (T_r) can be used to regulate pumps as well. The feedback mechanism can usually work well when there are not too many controllers with coupling control aims. Unfortunately, there is severe nonlinear hydraulic coupling between the flow rates of the valves and pumps in a complex chilled water distribution system. For instance, when one of the valves is adjusted to a new set point, the flow rates of the other valves would be influenced instantly. Then, the PID controllers must act on their valves to keep their own set points.

The adjustments of the valves would thereafter influence each other continuously, which would cause hydraulic oscillations in the pipe network. This phenomenon can significantly deteriorate the control performance. When the variable-speed pumps are also involved in this control process, the hydraulic oscillations would be aggravated. Sometimes, hydraulic oscillations may cause the water hammer in the pipe network, which can lead to leaks or the rupturing of the pipes. To mitigate the hydraulic oscillations, a trade-off between control quality and control stability has to be made for the feedback control methods.
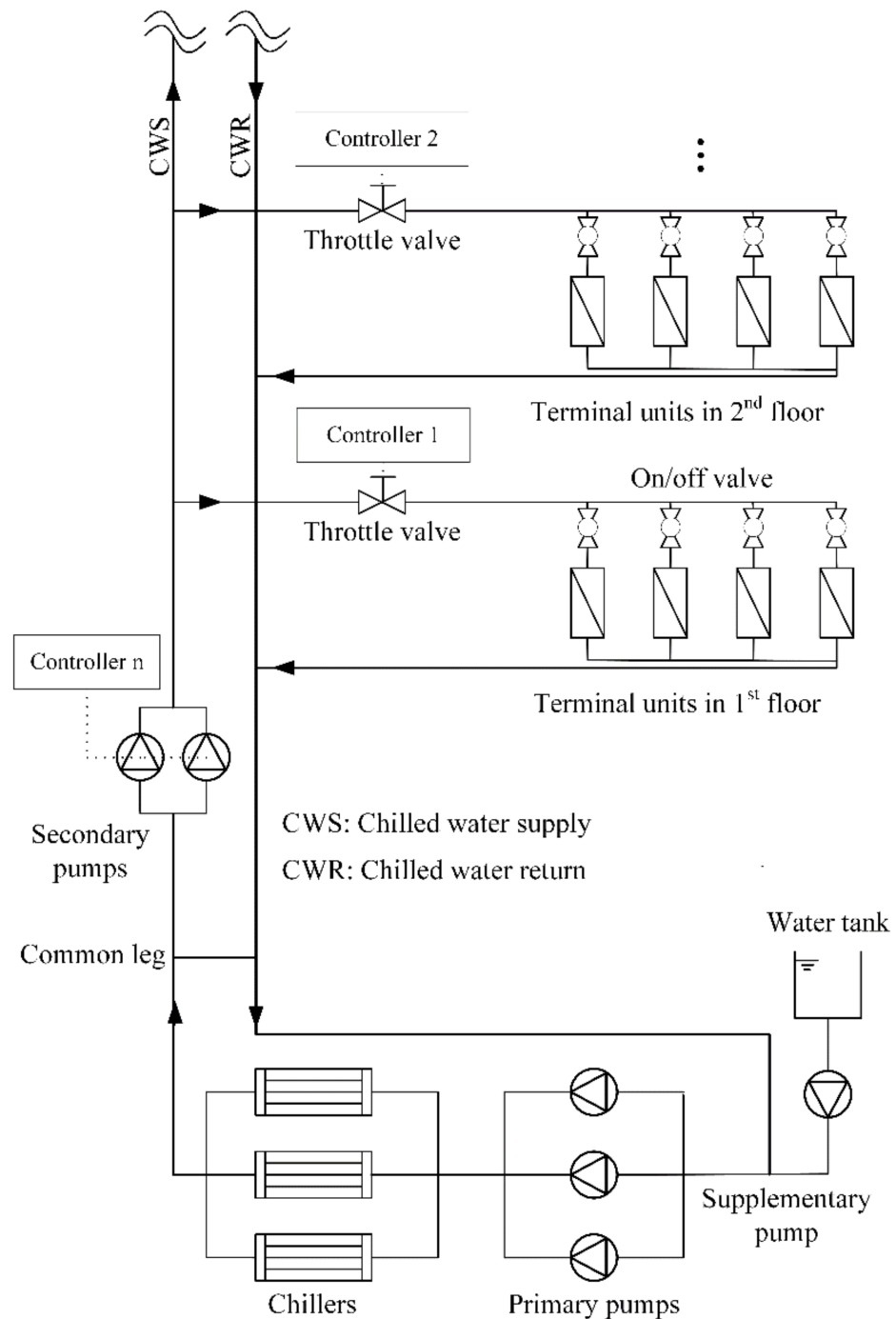

Figure 1. A typical configuration of a chilled water distribution system.

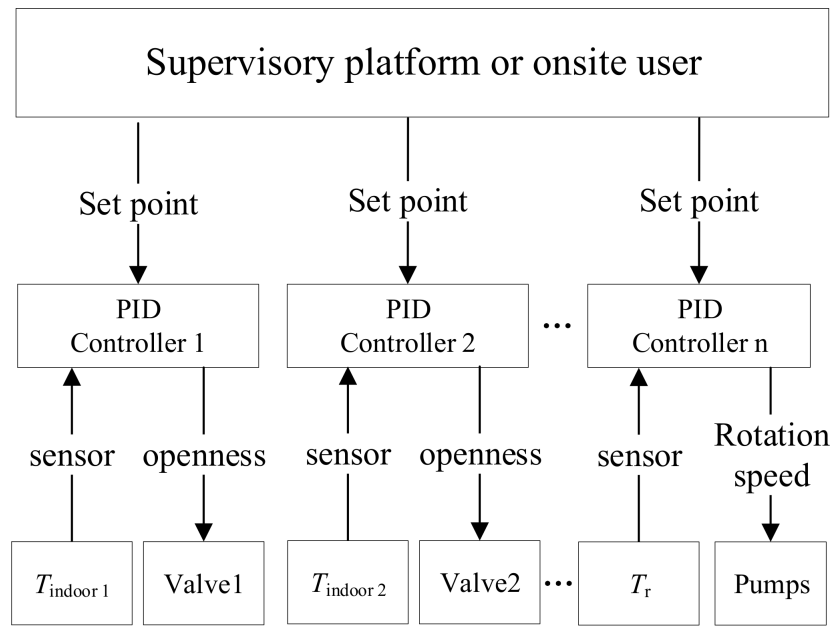**Figure 2.** A schematic control diagram of a typical PID control method.

2.3. Model Predictive Control Method

A new MPC method is introduced here, which is intrinsically immune to hydraulic oscillation while regulating valves and pumps in a complex water distribution system. A schematic control diagram of the proposed MPC method is shown in Figure 3.
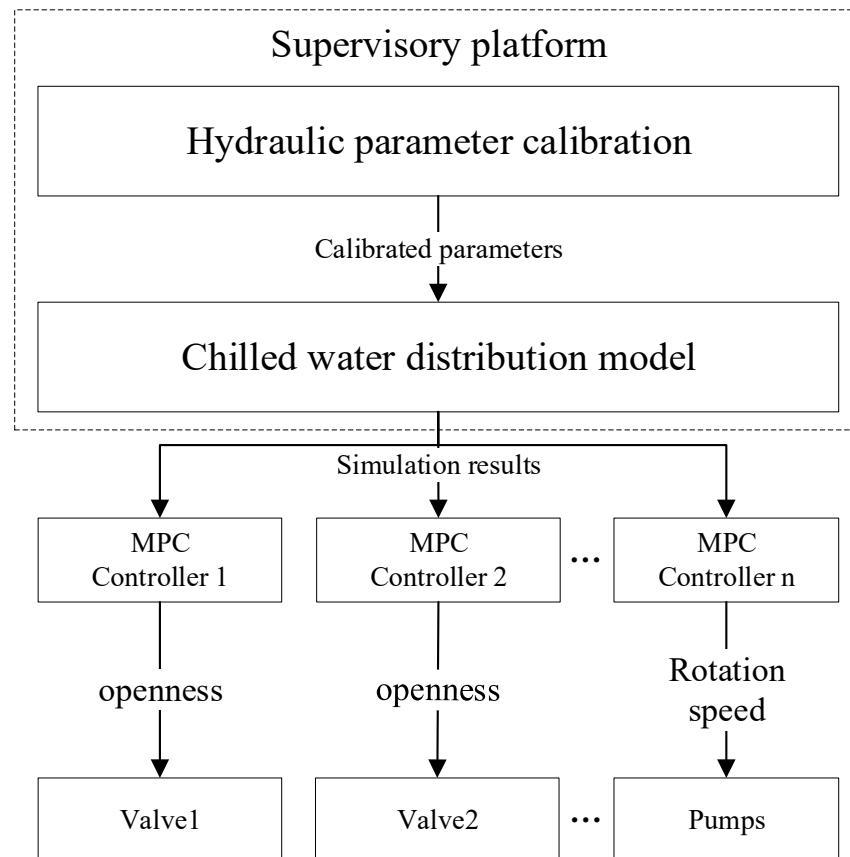

Figure 3. A schematic control diagram of the proposed MPC method.

In the proposed method, the valves and pumps are adjusted by so-called MPC controllers. There are no set-points for those MPC controllers. Instead, the simulation results from the chilled water distribution model are used for the MPC controllers to produce control signals to adjust the openness of valves or rotation speed of pumps. Without a feedback mechanism for the controllers, there is no possibility to produce hydraulic oscillation. To improve the accuracy of the simulation results, the parameters of the system model, such as hydraulic resistance of the pipes, chillers, and terminal units, should be calibrated regularly. Obviously, the proposed MPC control method is an intrinsically open loop control method. Therefore, the proposed method can be immune to any hydraulic oscillation. However, the effectiveness of the proposed method highly depends on an elaborate chilled water distribution model. A dedicated model for complex chilled water distribution system is presented in the next section. The details of the simulation results and process of the proposed method would be introduced in Section 5.

3. Chilled Water Distribution Model

The aim of the simulation is to obtain the required water pressure, flow rate, and temperature distribution in the pipe network. Then, the pumps and valves can be adjusted accordingly to supply proper water flow to the terminal units as demanded. The modeling for chilled water distribution system can be developed from two aspects: the hydraulic model and thermal model. As the water pressure waves in a pipe can propagate in sound speed, a chilled water system would reach hydraulic stability within a few minutes following one round of regulation. The calibration and simulation process can be performed adequately based on a static hydraulic model. On the other side, the supply water temperatures of the chillers are usually from 5 to 10 °C. The return water temperatures also change in a small range. Therefore, the adjustments of the valves and pumps depend mainly on the simulation results of the hydraulic model than that of the thermal model. The chilled water distribution modeling is focused on the hydraulic model with the following assumptions that can reduce the computational burden without significant decline of accuracy:

- The friction factors between chilled water and pipe inner surface are temperature independent.
- The chilled water is incompressible.
- There is no leakage along the pipes.
- The thermal losses from pipe insulation layer to ambient are neglected.

During hydraulic modeling, a chilled water distribution system can be treated analogous to an electric circuit [38]. Besides the pipe junctions, the chillers and terminal units which connect the supply and return pipes are regarded as the "nodes". The pipes with valves and fittings are regarded as the "branches".

3.1. Model Predictive Control Method

From the view of the hydronic distribution, the hydraulic behaviors of the chillers can be simplified as that of local hydraulic resistances. The relationship between a chiller's resistance R_{CH} and its water flow rate $\dot{V}_{CH}$ can be regressed by using the measured data of onsite meters. Then, the hydraulic characteristic of a chiller can be written as Equation (1):

$$R_{CH} = r_2 \cdot \left(\dot{V}_{CH} \right)^2 + r_1 \cdot \dot{V}_{CH} + r_0 \tag{1}$$

where r_0, r_1, and r_2 are the fitting coefficients which can be calibrated with a few pairs of $\left(\dot{V}_{CH}, R_{CH} \right)$. Considering that the coefficients r_0 and r_1 have far less influence on resistance than r_2, the coefficients r_0 and r_1 can often be neglected to reduce computation burden.

The supply water temperature of a chiller can be treated as an already known value from onsite temperature sensors or set temperature value of the chiller in operation, which can be written as Equation (2):

$$T^s = T_{CH}^{set} \tag{2}$$

where T^s is the supply water temperature of a chiller; and T^{set}_{CH} is the set value of the chiller in operation.

The primary pumps are often operated at constant speed. Then, the hydraulic characteristic of a primary pump can be given as Equation (3):

$$\Delta H_{P1} = \rho g \left[k_2 \left(\dot{V}_{P1} \right)^2 + k_1 \left(\dot{V}_{P1} \right) + k_0 \right] \tag{3}$$

where ΔH_{P1} is the water head of the pump; $\dot{V}_{P1}$ is the water flow rate of the pump; k_0, k_1 and k_2 are the fitting coefficients which are usually provided by the pump manufacturer; Subscript "P1" indicates a primary pump.

At the inlet of the primary pump, there are often a supplementary pump and a water tank to provide a designed static pressure point in case of water leakage or vaporization. Then, the return water pressure P^r at the inlet of the primary pumps can be given as Equation (4):

$$P^r = P_{set} \tag{4}$$

where P_{set} is the designed static pressure.

The secondary pumps are usually operated at variable speed. The hydraulic characteristic of a variable-speed pump can be given as Equation (5):

$$\begin{cases} \Delta H_{P2} = \rho g \left[k_2 \left(\dot{V}_{P2} \right)^2 + k_1 \left(\dot{V}_{P2} \right) \left(\frac{n_{P2}}{n^0_{P2}} \right) + k_0 \left(\frac{n_{P2}}{n^0_{P2}} \right)^2 \right] \\ \left(\frac{n_{P2}}{n^0_{P2}} \right) = \left(\frac{Fr_{P2}}{Fr^0_{P2}} \right) \end{cases} \tag{5}$$

where n_{P2} is the current rotation speed of the pump; n^0_{P2} is the rated rotation speed of the pump; Fr_{P2} is the operation frequency corresponding to n_{P2}; Fr^0_{P2} is the rated operation frequency corresponding to n^0_{P2}; k_0, k_1, and k_2 are still the fitting coefficients of the pump.

3.2. Terminal Unit and Valve

The terminal units in a chilled water system can also be treated as local resistances as that of the chillers. In the calibration process, r_0, r_1, and r_2 are still the fitting coefficients for hydraulic resistance of a terminal unit. However, the flow rate of a terminal unit should be regulated to fulfill its customers' cooling energy demand. In the simulation process, the terminal units should be treated as nodes with required mass flow rates $\dot{m}_{TU}$, which is given as Equation (6):

$$\dot{m}_{TU} = \frac{Q_{TU}}{c_p \left(T^s_{TU} - T^r_{TU} \right)} \tag{6}$$

where Q_{TU} is the predicted cooling load of the terminal unit; T^s_{TU} is the supply water temperature of the terminal unit; and T^r_{TU} is the return water temperature of the terminal unit.

Q_{TU} is usually estimated from a cooling load prediction software tool. Considering that the insulation layers of the chilled water pipes are often effective to prevent the heat transferring to ambient, T^s_{TU} is approximately equal to the supply water temperature of the chillers. T^r_{TU} depends on the onsite conditions and effectiveness of the terminal unit. For instance, a coil in good condition can reach the designed ΔT syndrome with required mass flow rates $\dot{m}_{TU}$. The designed ΔT is normally provided by the manufactory, such as 5.0 °C. Then, T^r_{TU} can be selected to be $\left(T^s_{TU} - 5 \right)$. When the required mass flow rate of a terminal unit had been determined by Equation (6), the corresponding pressure drop of this terminal unit can be obtained by the simulation process.

The pressure drop of a throttle valve ΔP_V can be estimated from its hydraulic characteristics as Equation (7):

$$\Delta P_V = \left(\frac{\rho}{\rho_v} \right) \left(\frac{\dot{V}_V}{K_v} \right)^2 \tag{7}$$

where $\dot{V}_V$ is the water flow rate of the valve; ρ_v is the water density at 16 °C; ρ is the water density by the valve; K_v is the flow coefficient of the valve, which can be given as Equation (8):

$$K_v = f(\varphi) \tag{8}$$

where φ is the openness of the valve; and the relation between K_v and φ is provided by the manufacturer.

When the required valve's pressure drop and flow rate have been obtained by hydraulic simulation, the required openness of the valve can be obtained by Equation (7) and Equation (8).

3.3. Pipe Network

The hydraulic model of a chilled water pipe network can also be treated analogous to that of an electricity circuit [38]. Specifically, the pressure drop, flow, and pipeline resistance characteristic coefficient can be regarded as the voltage, current, and electric resistance. Considering the topology of a pipe network layout, k is the total branch number, and $(n + 1)$ is its total node number. Then, the associated matrix A and the basic circuit matrix B of the pipe network can be obtained from graph theory.

According to the Kirchhoff's current law, it can be written as Equation (9):

$$A \cdot \dot{V}_b = 0 \tag{9}$$

where $\dot{V}_b$ is the flow rate column vector of each branch.

From the Kirchhoff's voltage law, it can be written as Equation (10),

$$B \cdot \left(R_b - \rho g H_p + \rho g Z_b \right) = 0 \tag{10}$$

where R_b is the resistance column vector of each branch; H_p is the pump head column vector of each branch; and Z_b is the height difference column vector for each branch.

The resistance of a pipe can be estimated by the equation of Darcy [39] as Equation (11):

$$R = f \cdot \frac{8 \rho l \left(\dot{V} \right)^2}{\pi^2 (d)^5} \tag{11}$$

where R is the resistance of the pipe; l is the length of the pipe; d is the inner diameter of the pipe; $\dot{V}$ is the volume flow rate of the pipe. f is friction factor of the pipe, which can be estimated by the equation of Colebrook–White [40] as Equation (12),

$$\frac{1}{\sqrt{f}} = -2lg \left(\frac{\varepsilon/d}{3.76} + \frac{2.51}{Re \sqrt{f}} \right) \tag{12}$$

where ε is the absolute roughness of the inner surface of the pipe; Re is the Reynold number.

4. Calibration Method

4.1. Calibration Model

The resistances of the pipes, chillers, and terminal units, which are necessary parameters for hydraulic simulations, must be calibrated firstly. A valid calibration model can find a set of optimal resistance values by the measurements. Based on the calibrated parameters, the simulation model can reach an acceptable match between the measured and the estimated data. Considering the non-analytical and non-smooth characteristics of the decision variables, the calibration model in the paper is also developed with an optimization method, as shown in Table 1.

Table 1. The calibration model.

Objective Function	$Min \sum\limits_{w=1}^{W} \left[\sum\limits_{m=1}^{M} \|P_m^e - P_m^o\| + \sum\limits_{n=1}^{N} \|\acute{V}_n^e - \acute{V}_n^o\| \right]$	(13)
Decision variable	R_i, R_j, ε_k	
S.T.	$R_{i,min} \leq R_i \leq R_{i,max}$	(14)
	$R_{j,min} \leq R_j \leq R_{j,max}$	(15)
	$\varepsilon_{k,min} \leq \varepsilon_k \leq \varepsilon_{k,max}$	(16)
	$P_{m,min}^e \leq P_m^e \leq P_{m,max}^e$	(17)
	$\acute{V}_{n,min}^e \leq \acute{V}_n^e \leq \acute{V}_{n,max}^e$	(18)

In the objective function, Equation (13), P_m^e and P_m^o are the estimated and observed pressure values, respectively; $\acute{V}_n^e$ and $\acute{V}_n^o$ are the estimated and observed volume flow rate values, respectively. Superscript "e" indicates estimated value; Superscript "o" indicates the observed value. There are M pressure meters and N flow meters onsite. There are a total of W times for calibration. The decision variable R_i is the hydraulic resistance of the chiller i. The decision variable R_j is the hydraulic resistance of the terminal unit j. The decision variable ε_k is the inner surface roughness of the pipe k. Equations (14)–(18) are constraints, where subscript min indicates the minimum feasible value, max indicates the maximum feasible value. The limits of the decision variables (R_i, R_j, ε_k) are the recommended engineering values. The feasible ranges of pressure and flow rate (P_m^e, $\acute{V}_n^e$) are within the capacities of the pumps and influenced by the arrangement of the local equipment.

4.2. Genetic Algorithm Solution

The genetic algorithm (GA) is employed to get a global optimization result considering the non-analytical and non-smooth properties of a pipe network hydraulic model. During the GA processing, the decision variables will be discretized in their range. For instance, the roughness of the pipes ε_k can be discretized into 2^{10} different values between its upper limit (i.e., 1 mm) and lower limit (i.e., 0.01 mm). For instance, we made the roughness of the pipes ε_k discrete into 2^{10} different values between its upper limit (i.e., 1 mm) and lower limit (i.e., 0.01 mm). The resolution of $\Delta\varepsilon_k$ can be obtained by Equation (19):

$$\Delta\varepsilon_k = \frac{\varepsilon_{k,max} - \varepsilon_{k,min}}{2^{10} - 1} = 9.677 \times 10^{-4}(mm) \tag{19}$$

Such a resolution $\Delta\varepsilon_k$ may be precise enough to meet the calibration requirement of most chilled water systems. The other two decision variables R_i, R_j can be discretized similarly. For instance, $R_{i,min}$ and $R_{i,max}$ are set to be 1 kPa and 80 kPa, respectively. $R_{j,min}$ and $R_{j,max}$ are set to be 1 kPa and 50 kPa, respectively. After R_i, R_j are calibrated, the fitting parameters r_0, r_1, and r_2 can be regressed as Equation (1). Figure 4 shows the scheme of the GA algorithm for the calibration model. The number of generations are defined as variable "Gen". The GA algorithm would iterate until the value of "Gen" reaches the maximum number "MaxGen". Due to the sophisticated mechanisms of the GA algorithm, this paper does not discuss the impact of the population size, probability of crossover, and probability of mutation on the algorithm.
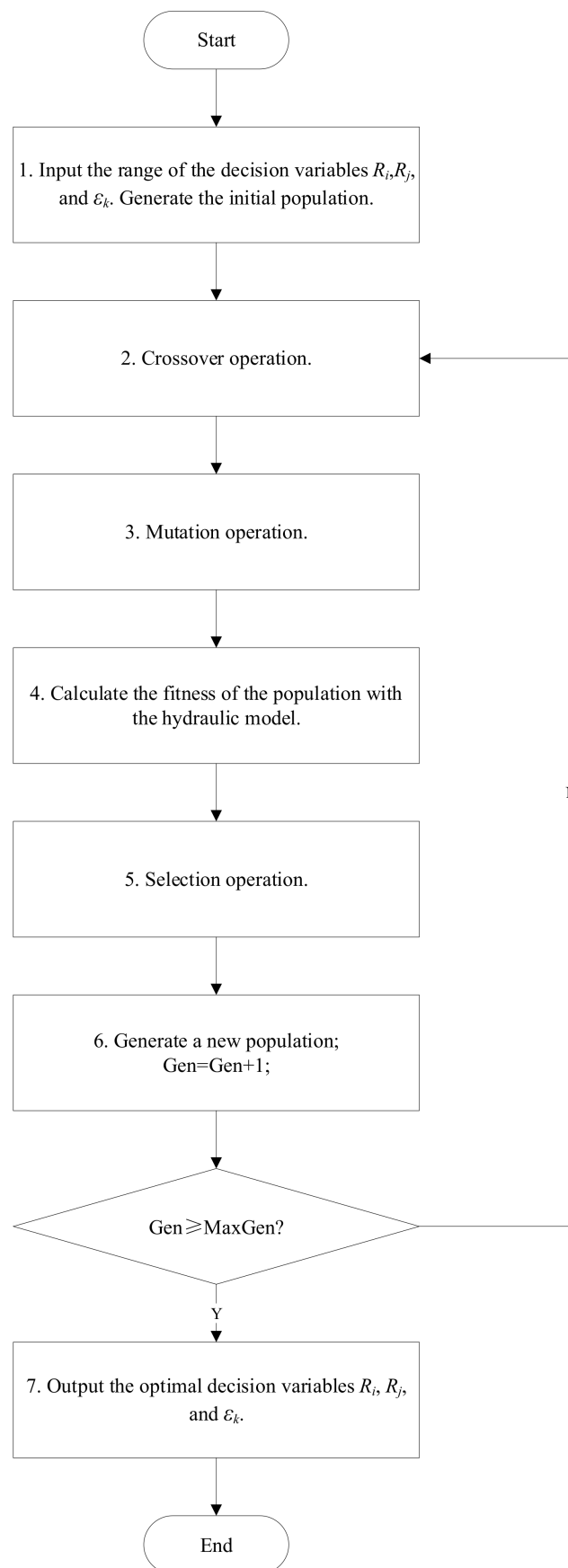
Figure 4. Scheme of the GA algorithm.

5. Design and Operation

Based on the advanced automation system of the chilled water system, the design of the local MPC controllers and the onsite operation approach are presented in detail in this section.

5.1. Local MPC Controller Design

The proposed MPC controllers are used to adjust the openness of the throttle valves and variable-speed pumps. With regard to an MPC controller of a valve, the openness can be calculated by its pressure drop and flow rate. According to Equation (7), it is rewritten as Equation (20):

$$K_v = \dot{V}_V \sqrt{\left(\frac{\rho}{\rho_v}\right)\left(\frac{1}{\Delta P_V}\right)} \tag{20}$$

Combining Equation (20) with Equation (8), it is given as Equation (21):

$$\varphi = f^{-1}\left(\dot{V}_V \sqrt{\left(\frac{\rho}{\rho_v}\right)\left(\frac{1}{\Delta P_V}\right)} \right) \tag{21}$$

where f^{-1} is the reverse function of Equation (8); the relation between φ and K_v depends on the hydraulic characteristic of the valve. It is often expressed as a nonlinear function as Equation (22),

$$\varphi = a_2 \left(\frac{\dot{V}_V}{\sqrt{\Delta P_V}} \right)^2 + a_1 \frac{\dot{V}_V}{\sqrt{\Delta P_V}} + a_0 \tag{22}$$

where a_1 and a_0 are the fitting coefficients provided by the manufacturer.

When the simulation results of ΔP_V and $\dot{V}_V$ are obtained by the proposed hydraulic model, the MPC controller can calculate the expected openness of the valve instantly by Equation (21) or Equation (22). Then, the openness of the valve can be adjusted by an accurate signal from its actuator.

With regard to an MPC controller of a variable-speed pump, the rotation speed can also be calculated by its water head and flow rate. According to Equation (5), it is given as Equation (23),

$$\left(\frac{n_{P2}}{n_{P2}^0}\right) = \frac{1}{2a_P}\left(-b_P \pm \sqrt{b_P^2 - 4a_P c_P}\right), \tag{23}$$

where a_P, b_P, and c_P are the factors as follows:

$$a_P = \rho g k_0 \tag{23a}$$

$$b_P = \rho g k_1 \acute{V}_{P2} \tag{23b}$$

$$c_P = \rho g k_2 \dot{V}_{P2}^2 - \Delta H_{P2} \tag{23c}$$

Since the pump characteristic curve (ΔH_{P2}-$\dot{V}_{P2}$) is an inverted parabola, k_0 is a negative number, and so is a_P. Therefore, the $\pm$ sign in Equation (23) means that the positive sign is for all points to the right of the curve maxima, while the negative sign applies to points to the left of it. In some situations, there are two possible rotation speeds corresponding to the same water head of the pump. It can lead to physical instabilities for the pump to alternate between two rotation speeds. The MPC controller of pump should choose the value closer to the current rotation speed.

Similarly, when the simulation results of ΔH_{P2} and $\dot{V}_{P2}$ are obtained by the proposed hydraulic model, the MPC controller can calculate the expected operation frequency of the pump by Equations (23) and (5). Then, the operation frequency of the pump can be adjusted by an accurate signal from its invertor.

5.2. Real-Time Regulation Approach

With the help of automation and information technologies, such as the Building Information Modeling (BIM) system, Building Automation (BA) system, Cloud Service (CS) and Remote Control (RC), the proposed MPC method can be implemented smoothly. The real-time control process is usually following the hourly cooling load prediction. Therefore, the period of the real-time regulations on the valves and pumps in a chilled water system is also 1 h accordingly. To realize the proposed method, there are four successive steps in a round of regulation, as shown in Figure 5:
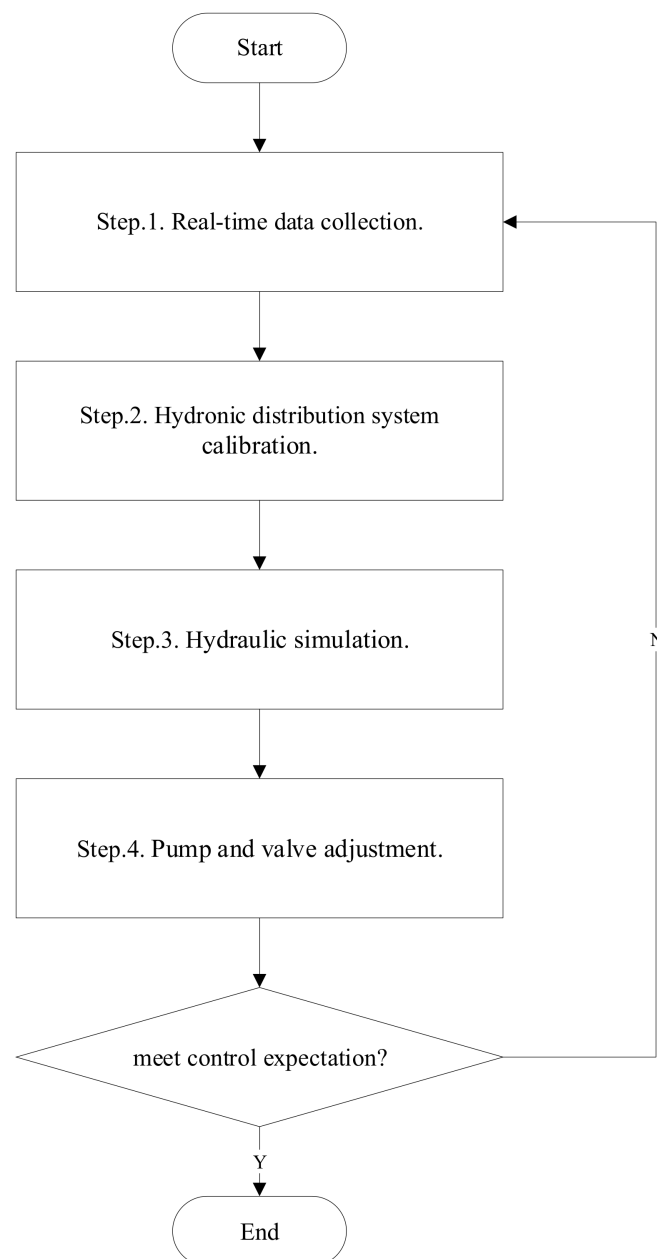
(1) Real-time data collection

Figure 5. Flow chart of an on-site hydraulic regulation method in a chilled water system.

The current hydraulic state of the chilled water system should be collected by an effective data access system, such as the Building Automation (BA) system. The network layout, location of chillers and terminal units, integrity of pipes and pumps, etc. can be recorded by a database system, such as BIM or CAD-based tools. The valid data are

treated as the initial and boundary conditions, which are the foundation for the hydraulic calibration and simulation.

(2)   Hydronic distribution system calibration

The onsite meters are installed at selected positions of the water pipe network. For instance, the entrance of each floor, the inlet and outlet of the chillers, valves, pumps, and some key terminal units are usually selected to install pressure meters, flow rate meters, or temperature sensors. Based on the measured data, the resistance of pipes, chillers, and terminal units can be calibrated by the proposed calibration method. Generally, the accuracy of a calibration model is positively correlated with the amount of valid data. The calibration process can be performed in Cloud Service or the local server. CS is more adapted to serve many buildings simultaneously. It is more economic and efficient in recent years to deploy all algorithms and operation data in the public cloud.

(3)   Hydraulic simulation

With the calibrated parameters in step (2), an hourly hydraulic simulation on the chilled water system can be carried out based on the hourly cooling load prediction. The pressure drops and flow rates of the throttle valves and the water heads and flow rates of the variable-speed pumps are calculated to achieve hydraulic balance for terminal users in different floors. The simulation process can also be performed in CS. Then, the simulation results can be transferred to the MPC controllers via internet or local network.

(4)   Pump and valve adjustment

With the values of pressure and flow rate from the hydraulic simulation, the MPC controller can produce the corresponding control signals to adjust valves or pumps. In order to avoid the hydraulic oscillation, all valves and pumps should be adjusted to the latest values simultaneously. To fulfill this task, an RC system can be used to adjust the pumps and valves in different locations.

After a round of regulation, water flow in pipes would stabilize in one or two minutes. Then, the control effect would be evaluated instantly. The next round of calibration process would use the collected pressures and flow rates as new input data to obtain more accurate calibration parameters. Because the errors in the calibration and simulation process would be improved in the next round of regulation, sometimes, the onsite regulation had to be performed for 2–3 rounds to meet control expectation as close as possible. Generally, the errors between observed and expected flow rates are good criteria to determine whether the control expectation has been met. The criterion for the onsite regulation is given as Equation (24):

$$\epsilon_n = \frac{\left| \acute{V}_n^e - \acute{V}_n^o \right|}{\acute{V}_n^e} \leq \epsilon_{max}, \forall n \in N \tag{24}$$

where $\acute{V}_n^e$ is the expected flow rate; $\acute{V}_n^o$ is the observed flow rate of onsite meter; ϵ_{max} is the allowable relative error; ϵ_n is the relative error of flow meter n. Subscript n is the index of the flow meter; N is the total assembly of the flow meters.

6. Case Study

To validate the proposed MPC method, the control system of the chilled water system in a hotel in Shanghai was retrofitted in April of 2019. The topology diagram of the chilled water distribution system is shown in Figure 6. There are 22 floors in this high-rise building with several Air Handling Units (AHUs) in each floor. To overcome the severe hydraulic imbalance among different floors, 22 throttle valves with MPC controllers are installed in the supply water pipe at the entrance of each floor. There are two identical chillers in operation. The rated cooling capacity of the chiller is 865.6 kW, and the rated power consumption is 245.2 kW. The designed temperature of chilled water supply/return is 7/12 °C. The rated volume flow rate of the primary pump is 90.0 m^3/h, and the rated water head is 27.9 mH$_2$O. There are six identical secondary pumps with a rated volume flow rate as 55.0 m^3/h and a rated water head as 30.7 mH$_2$O. There are six identical secondary

pumps with a rated volume flow rate of 55.0 m^3/h and a rated water head of 30.7 mH$_2$O. Usually, there are three primary pumps and four secondary pumps in operation. The primary pumps are running at a constant speed. The secondary pumps are variable-speed pumps with a shared MPC controller. There are also 27 water pressure meters and 24 flow rate meters installed at the inlets or outlets of chillers and valves. The resolutions of water pressure meters and flow meters are 0.1 kPa and 0.1 m^3/h, respectively.

Figure 6. Topology of the chilled water distribution system.

The lengths and diameters of pipes and locations of the chillers, valves, pumps, and terminal units had been obtained from the CAD drawings of the project. To simulate the water distribution system, two chillers, 22 throttle valves, three primary pumps, six secondary pumps, 202 terminal units, and 946 pipes are involved in the simulation model. The adjustments of valves and pumps are performed hourly according to the hourly cooling load prediction. The cooling load prediction was provided from a third-party software based on the well-known tool "Energy-plus", which considered local climate and occupants

activities, etc. Then, we can begin a round of regulation, for instance, at 12:00 p.m. on a typical summer day (22 July 2018).

(1)   Step 1.

The real-time observed data of 27 pressure meters and 24 flow meters were collected every 30 s by wireless signals. Then, 120 groups of observed values of pressure and flow rate can be collected in an hour. However, the hydraulic conditions between two rounds of adjustments (in an hour) were usually similar. Then, the collected data each 15 min were averaged as only one sample for calibration. In this case, the observed date in recent 72 h (288 samples) was used to calibrate the hydraulic resistances of pipes, chillers, and AHUs. The primary pumps are running at a constant speed (50 Hz), while the secondary pumps are running at variable speed according to the control strategy. The hydraulic characteristic curves of the primary and secondary pumps are shown in Figures 7 and 8, respectively.
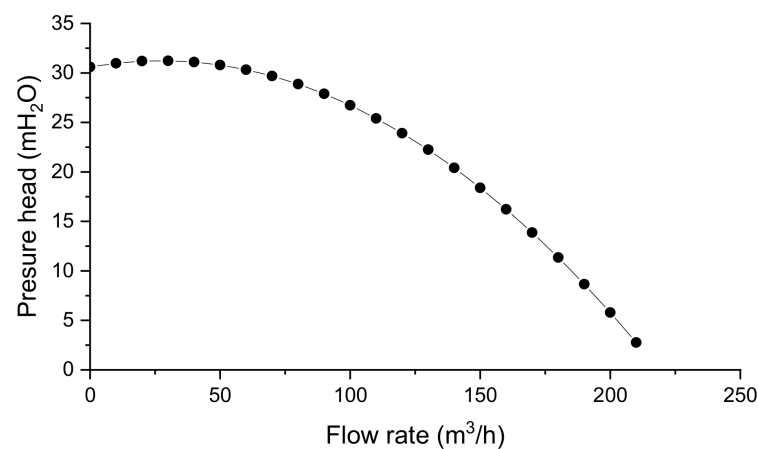
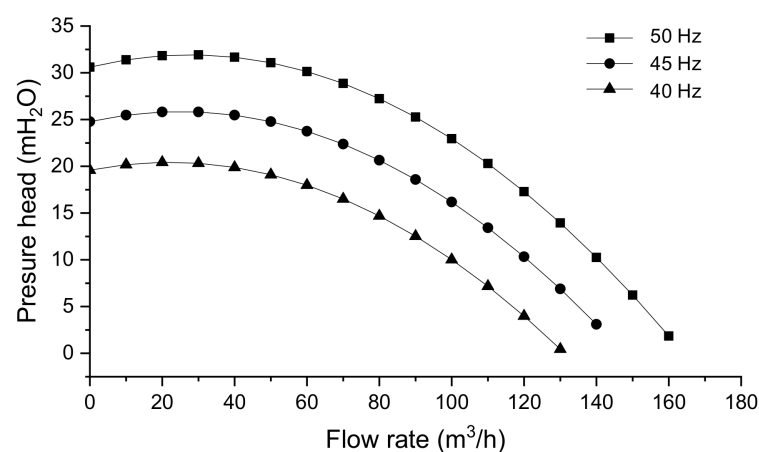**Figure 7.** The hydraulic characteristic curves of the primary pump.

Figure 8. The hydraulic characteristic curves of the secondary pump.

(2)   Step 2.

In step 2, the hydraulic resistances of the chillers and terminal units, and the roughness of the inner surface of the pipes were calibrated by the proposed method. According to Equation (13), $W = 288$, $M = 27$, and $N = 24$. The initial values of all the roughness of the pipes were set as 100 (μm). The initial values of resistance coefficients of all chillers (r_0, r_1, r_2) were set as (0, 0, 0.80). That of all terminal units was set as (0, 0, 8.0). Coefficients r_0 and r_1 were neglected for simplification. Using the GA algorithm, the decision variables were coded into 100 chromosomes for the initial population. In addition, the "MaxGen" was set

to 100 in the case. The calibrated roughness values of all pipes are shown in Figure 9. The average roughness of all pipes is 141.1 (μm). The calibrated resistance coefficient values of all terminal units are shown in Figure 10. The average resistance coefficient r_2 of all terminal units is 25.8. The calibrated local resistance coefficient r_2 of 2 chillers are 0.940 and 0.958, respectively.
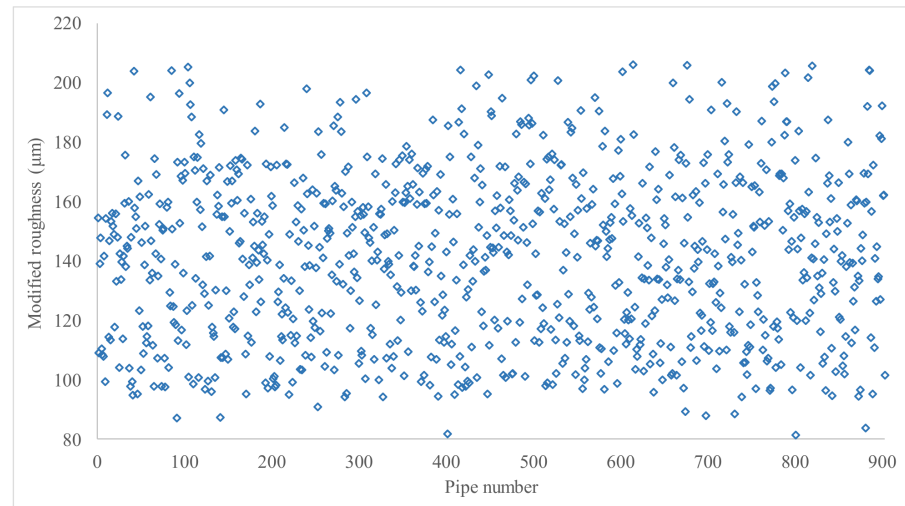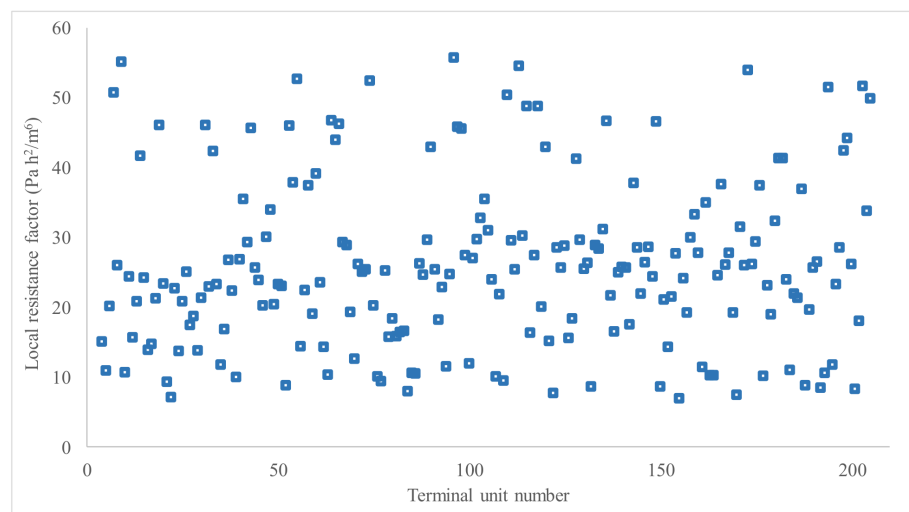

Figure 9. The calibrated value ε_k of all pipes.

Figure 10. The calibrated value r_2 of all terminal units.

(3)   Step 3.

With the latest calibrated parameters, the simulation step can be performed based on the current cooling load prediction. The required flow rates of terminal units can be obtained by Equation (6). Then, the water pressure and flow rate distribution in the pipe network can be simulated accordingly. The simulation program is developed by the authors of this paper on the Microsoft Visual studio 2017 platform. One simulation took less than 2 min. The simulation results can be illustrated clearly as color-coded maps according to the construction CAD drawings. For simplicity, not all 24 simulation results from 12:00 a.m. to 11:00 p.m. are illustrated there. The simulation results of the water pressure and flow rate distribution at 12:00 a.m. are shown in Figures 11 and 12, respectively.
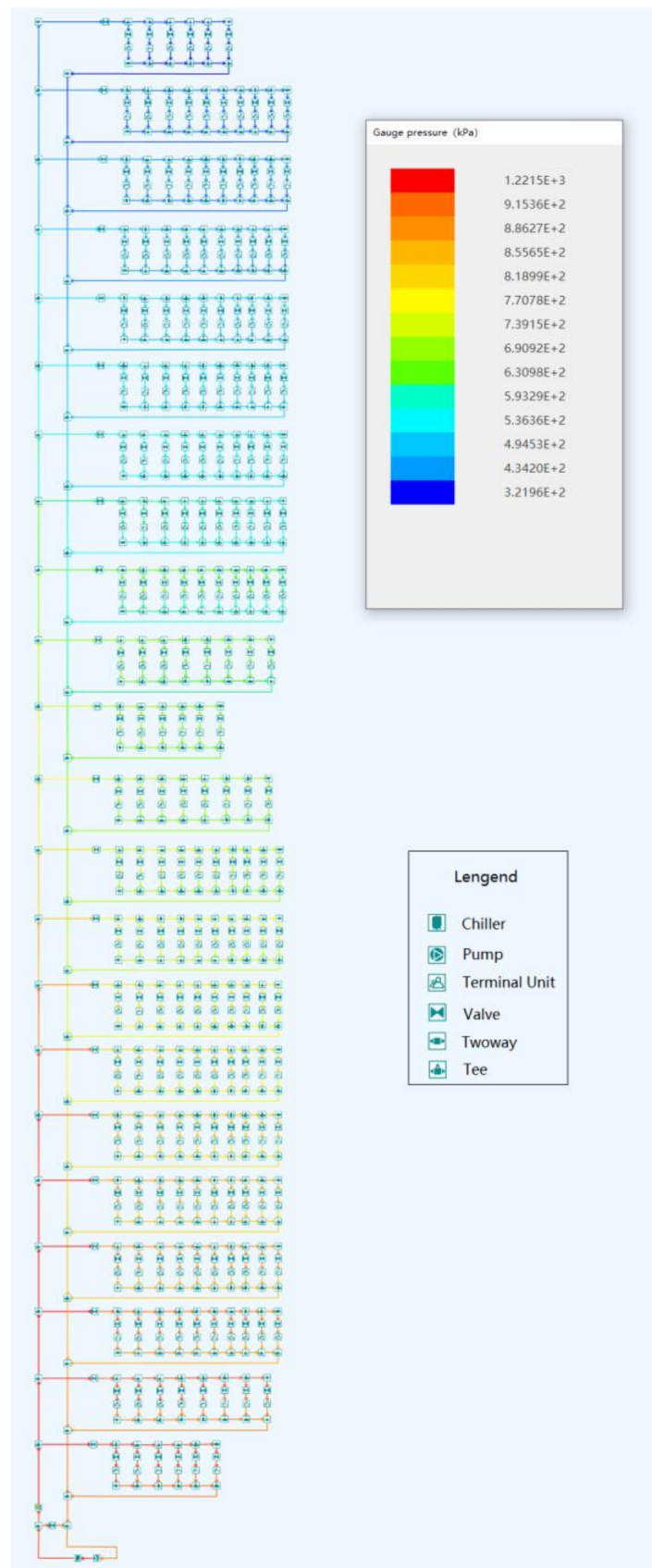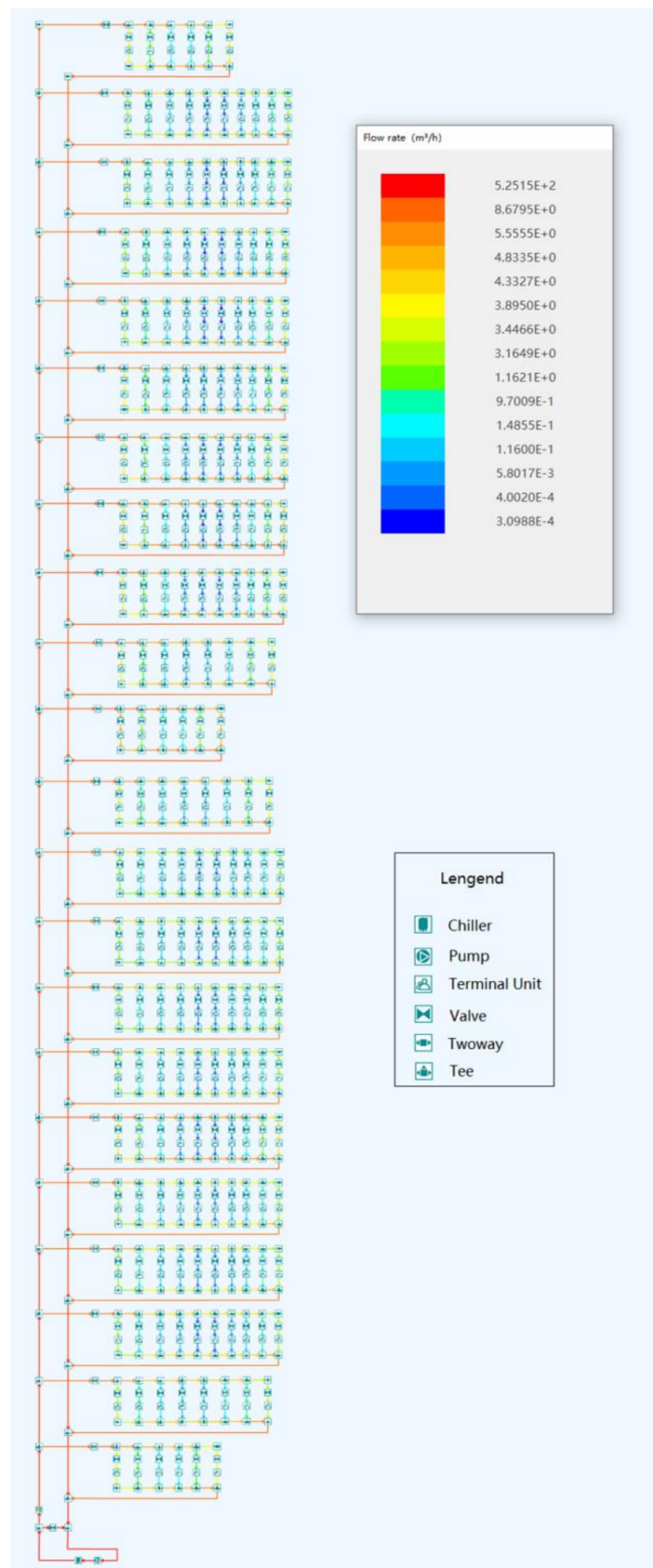
Figure 11. Water pressure distribution.

Figure 12. Water flow rate distribution.

The required pressure drops and flow rates of the throttle valves are shown in Table 2. The simulation results of the valves would be transferred to the MPC controllers via wireless signal either.

Table 2. The required pressure drops and flow rates of the throttle valves.

Valve Number	Pressure Drop (Pa)	Flow Rate (m³/h)	Openness (%)
1	264,856	8.46	10.4
2	231,223	9.00	11.5
3	200,427	9.54	12.5
4	175,303	7.79	13.2
5	150,997	7.59	14.6
6	115,666	11.12	18.3
7	108,372	7.66	14.2
8	92,802	6.85	13.8
9	77,022	6.73	14.9
10	62,748	6.63	16.2
11	43,731	9.45	27.7
12	23,191	9.67	38.9
13	24,461	13.00	50.9
14	10,462	10.40	62.2
15	11,598	11.54	59.9
16	6139	10.58	75.5
17	5360	9.82	75.0
18	3698	9.28	85.3
19	3382	8.90	85.6
20	2783	8.68	91.9
21	1996	8.57	99.9
22	3879	10.25	92.0

The required pressure head and flow rate of each secondary pump is 31.05 mH$_2$O and 201.5 m^3/h, respectively. To save electricity as much as possible, the pressure head of the secondary pump should be set at a low value for which least one of the 22 throttle valves consumes a water pressure drop of no more than 2.0 kPa. The lowest pressure head of the secondary pump can be obtained in 2–3 tries.

(4)   Step 4.

When the MPC controllers of the 22 valves and six pumps obtained the latest simulation results, the openness of valves and frequency of the pumps can be adjusted by Equations (22) and (23), respectively. The openness of the valves at 12 o'clock is also shown in Table 2. The frequency of the secondary pump is 46.846 Hz accordingly.

From above steps 1 to 4, a round of regulation at 12 a.m. was accomplished. After 3–5 min of this regulation finished, the observed data of the flow meters were used to determine whether the control expectation has been met according to Equation (24). As shown in Figure 13, the maximal relative error between observed and expected flow rates is less than 1.0%. It indicated that the control aim had been achieved after this round of regulation. The next round of regulation would be performed according to the latest cooling load prediction at 1:00 p.m. During the regulations by the proposed MPC method, the hydraulic oscillations in the chilled water system had been eliminated. Considering the large thermal inertia of the building, the hourly regulations are usually enough for the chilled water system in such a 22-floor hotel.
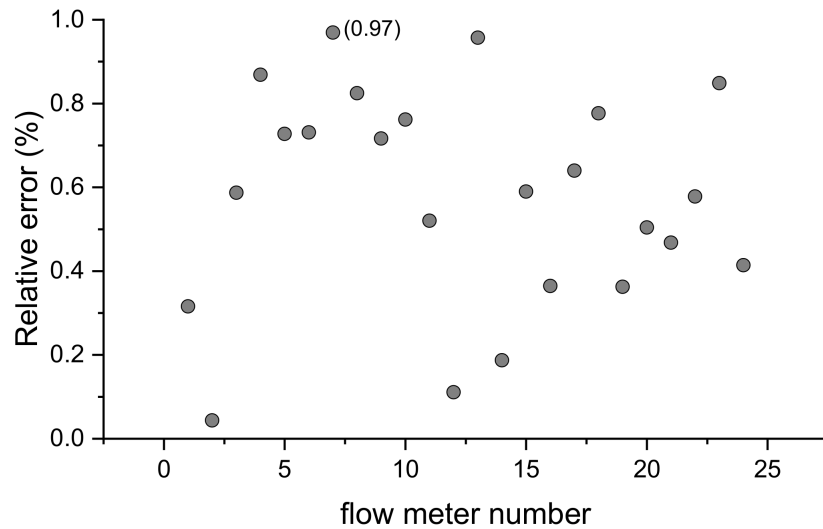
Figure 13. Relative error between observed and expected flow rates.

Furthermore, the dynamic hydraulic imbalance is almost eliminated after the proposed regulations. The hydraulic balance can significantly improve the system efficiency and hotel guests' comfort. In a conventional PID control method, the flow rate of the chilled water is regulated to fulfill the cooling demand of the least favorable circulating loop. The chilled water systems are often involved in a large flow rate and degrading ΔT syndrome in most PID-based control systems. Then, the terminal units in most floors are in an over-flow state, which causes excessive thermal waste and electricity consumption of the pumps. To evaluate the energy saving effects of the proposed (MPC) method, the hourly electricity consumed by the circulation pumps are simulated in conditions of the proposed method and the conventional method, respectively. The hourly simulation results in a typical summer day are shown in Figure 14. In this case, the average electricity saving of the proposed MPC method is as high as 23.3% in 24 h.
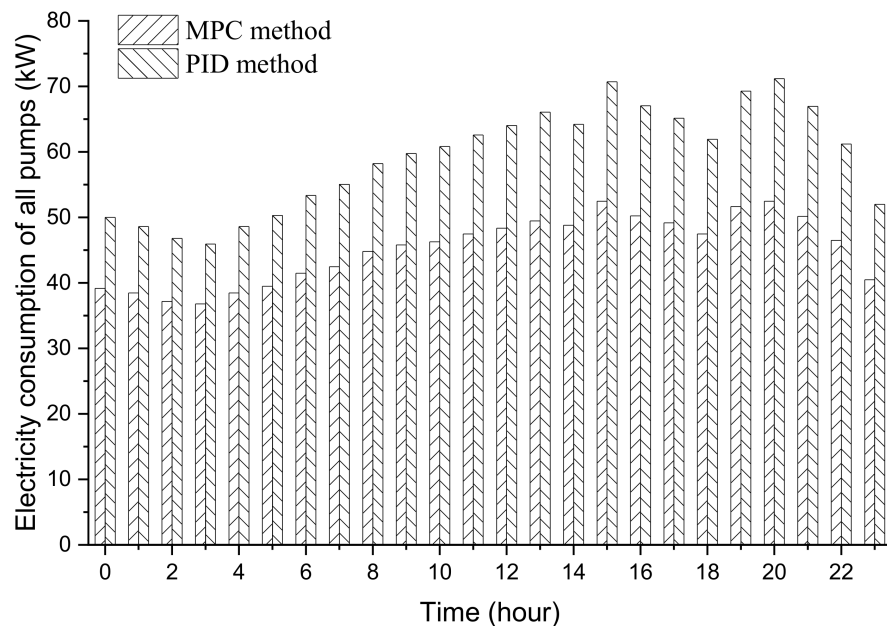

Figure 14. The hourly simulation results by the MPC method and the PID method.

It is noted that the electricity consumed by the chillers or pumps cannot be measured separately from other electricity devices by the onsite meters. Therefore, the measured electricity data of the pumps have to be absent in Figure 14. On the other hand, the actual energy consumptions of the terminal units in an over-flow state are not easy to estimate accurately in the simulation scenario by the conventional method. Therefore, the energy consumption of the chillers cannot be estimated accurately as well. As a rule of thumb, the real-life chillers can save more than 10% electricity consumption when the large flow rate and degrading ΔT syndrome are eliminated.

7. Conclusions

This paper proposed a safe and highly efficient MPC method for the chilled water system with the help of advanced automatic and information technologies including BIM, BA, CS, and RC. In a hotel of 22 floors, the proposed method is illustrated in detail about how to adjust valves and pumps step by step. The main conclusions of this paper are as follows:

(1) In a complex chilled water system with throttle valves and variable-speed pumps, a new MPC method is proposed for real-time operation to achieve dynamic hydraulic balance and immune hydraulic oscillation. By the proposed method, the MPC controller is designed instead of the conventional PID controller. A round of regulation encompasses four steps, which are (a) Real-time data collection; (b) Hydronic distribution system calibration; (c) Hydraulic simulation; and (d) Pump and valve adjustment. After a round of regulation, the control effect would be evaluated instantly. It can be improved to meet the control expectation as close as possible in the next round of regulation.

(2) A chilled water distribution model is developed to simulate a complex chilled water system in a high-rise building. The CAD drawings or BIM diagram of a real-life project can be used to produce the topology of the pipe network layout. The required water pressures and flow rates of the valves and variable-speed pumps can be obtained according to the cooling load demands by the proposed hydraulic model.

(3) A calibration method is presented with a dedicated optimization model. The genetic algorithm is used to search the global optimal values of the hydraulic resistances (R_i, R_j, ε_k) with non-analytical and non-smooth characteristics. The data collection system is used to provide the calibration model with real-time measured pressure and flow rate data.

(4) The proposed method got validated in a real chilled water system in a 22-floor hotel in Shanghai. The 22 throttle valves and six variable-speed pumps of the chilled water system were adjusted by the proposed MPC controllers in a typical summer day. The results indicated that the dynamic hydraulic balance was achieved without any hydraulic oscillations. The hourly electricity consumed by the circulation pumps are also compared between that of the proposed method and the conventional method. The average electricity savings of the proposed method is as high as 23.3% in a typical summer day.

Author Contributions: Y.Y. and N.Z. wrote this paper and developed the method. H.Z. and H.W. were responsible for data collecting and the validation of the proposed method. All authors have read and agreed to the published version of the manuscript.

Conflicts of Interest: The authors declare no conflict of interest.

References

1. International Energy Agency (IEA). Solar Heating and Cooling, Retrieved 14 February 2016. Available online: http://www.iea-shc.org/ (accessed on 16 May 2020).
2. Energy Information Administration (EIA). *Annual Energy Outlook 2012 Early Release*; Energy Information Administration (EIA): Washington, DC, USA, 2012.
3. Perez-Lombard, L.; Ortiz, J.; Pout, C. A review on buildings energy consumption information. *Energy Build.* **2008**, *40*, 394–398. [CrossRef]
4. Naidu, D.S.; Rieger, C.G. Advanced control strategies for heating, ventilation, air-conditioning, and refrigeration systems—An overview: Part I: Hard control. *Hvac R Res.* **2011**, *17*, 2–21.
5. Mirinejad, H.; Welch, K.C.; Spicer, L. *A Review of Intelligent Control Techniques in HVAC Systems*; Energytech/IEEE: Cleveland, OH, USA, 2012; pp. 1–5.
6. Wang, S.; Ma, Z. Supervisory and optimal control of building HVAC systems: A review. *Hvac&R Res.* **2008**, *14*, 3–32.
7. Yuan, S.; Perez, R. Multiple-zone ventilation and temperature control of a single-duct VAV system using model predictive strategy. *Energy Build.* **2006**, *38*, 1248–1261. [CrossRef]
8. Wang, S.; Xu, X.; Huang, G. Robust MPC for temperature control of air-conditioning systems concerning on constraints and multitype uncertainties. *Build. Serv. Eng. Res. Technol.* **2010**, *31*, 39–55.
9. Afram, A.; Janabi-Sharifi, F. Theory and applications of HVAC control systems e A review of model predictive control (MPC). *Build. Environ.* **2014**, *72*, 343–355. [CrossRef]
10. Afroz, Z.; Shafiullah, G.M.; Urmee, T.; Higgins, G. Modeling techniques used in building HVAC control systems: A review. *Renew. Sustain. Energy Rev.* **2018**, *83*, 64–84. [CrossRef]
11. Tashtoush, B.; Molhim, M.; Al-Rousan, M. Dynamic model of an HVAC system for control analysis. *Energy* **2005**, *30*, 1729–1745. [CrossRef]
12. Kohlenbach, P.; Ziegler, F. A dynamic simulation model for transient absorption chiller performance. Part I: The model. *Int. J. Refrig.* **2008**, *31*, 217–225. [CrossRef]
13. Chen, Y.; Treado, S. Development of a simulation platform based on dynamic models for HVAC control analysis. *Energy Build.* **2014**, *68*, 376–386. [CrossRef]
14. Jin, G.-Y.; Tan, P.-Y.; Ding, X.-D.; Koh, T.-M. Cooling coil unit dynamic control of in HVAC system. In Proceedings of the 2011 6th IEEE Conference on Industrial Electronics and Applications, Beijing, China, 21–23 June 2011; pp. 942–947.
15. Huang, G. Model predictive control of VAV zone thermal systems concerning bi-linearity and gain nonlinearity. *Control. Eng. Pract.* **2011**, *19*, 700–710. [CrossRef]
16. Hu, J.; Karava, P. Model predictive control strategies for buildings with mixed-mode cooling. *Build. Environ.* **2014**, *71*, 233–244. [CrossRef]
17. Viot, H.; Sempey, A.; Mora, L.; Batsale, J.C.; Malvestio, J. Model predictive control of a thermally activated building system to improve energy management of an experimental building: Part II—Potential of predictive strategy. *Energy Build.* **2018**, *172*, 385–396. [CrossRef]
18. Candanedo, J.A.; Dehkordi, V.R.; Stylianou, M. Model-based predictive control of an ice storage device in a building cooling system. *Appl. Energy* **2013**, *111*, 1032–1045. [CrossRef]
19. Ma, J.; Qin, J.; Salsbury, T.; Xu, P. Demand reduction in building energy systems based on economic model predictive control. *Chem. Eng. Sci.* **2011**, *67*, 92–100. [CrossRef]
20. Henze, G.P.; Kalz, D.E.; Liu, S.; Felsmann, C. Experimental analysis of model-based predictive optimal control for active and passive building thermal storage inventory. *Hvac&R Res.* **2005**, *11*, 189–213.
21. Karlsson, H.; Hagentoft, C.-E. Application of model based predictive control for water-based floor heating in low energy residential buildings. *Build. Environ.* **2011**, *46*, 556–569. [CrossRef]
22. Taylor, S.T. *Fundamentals of Design and Control of Central Chilled-Water Plants (SI)*; ASHRAE Learning Institute: Peachtree Corners, GA, USA, 2017.
23. Afram, A.; Janabi-Sharifi, F.; Fung, A.S.; Raahemifarb, K. Artificial neural network (ANN) based model predictive control (MPC) and optimization of HVAC systems: A state of the art review and case study of a residential HVAC system. *Energy Build.* **2017**, *141*, 96–113. [CrossRef]
24. Ascione, F.; Bianco, N.; de Stasio, C.; Mauro, G.M.; Vanoli, G.P. A new comprehensive approach for cost-optimal building design integrated with the multi-objective model predictive control of HVAC systems. *Sustain. Cities Soc.* **2017**, *31*, 136–150. [CrossRef]
25. Bi, Q.; Cai, W.-J.; Wang, Q.-G.; Hang, C.-C.; Lee, E.-L.; Sun, Y.; Liu, K.-D.; Zhang, Y.; Zou, B. Advanced controller auto-tuning and its application in HVAC systems. *Control. Eng. Pract.* **2000**, *8*, 633–644. [CrossRef]
26. Kusiak, A.; Li, M.; Zhang, Z. A data-driven approach for steam load prediction inbuildings. *Appl. Energy* **2010**, *87*, 925–933. [CrossRef]
27. Lixing, D.; Jinhu, L.; Xuemei, L.; Lanlan, L. Support vector regression and ant colony optimization for HVAC cooling load prediction. In Proceedings of the 2010 International Symposium on Computer Communication, Control and Automation (3CA), Tainan, Taiwan, 5–7 May 2010.
28. Chen, K.; Jiao, Y.; Lee, E.S. Fuzzy adaptive networks in thermal comfort. *Appl. Math. Lett.* **2006**, *19*, 420–426. [CrossRef]

29. Lu, H.; Jia, L.; Kong, S.Z.Z. Predictive functional control based on fuzzy T-S model for HVAC systems temperature control. *J. Control. Theory Appl.* **2007**, *5*, 94–98. [CrossRef]

30. Jacob, Y.C.-M. Statistical Modelling and Forecasting Schemes for Air-conditioning System. Ph.D. Thesis, The Hong Kong Polytechnic University, Hong Kong, 2008.

31. Ma, J.; Qin, S.J.; Li, B. Salsbury, Economic model predictive control for building energy systems. In Proceedings of the Innovative Smart Grid Technologies (ISGT), 2011 IEEE PES, Hilton Anaheim, CA, USA, 17–19 January 2011.

32. Ma, Z.; Wang, S. An optimal control strategy for complex building central chilled water systems for practical and real-time applications. *Build. Environ.* **2009**, *44*, 1188–1198. [CrossRef]

33. Ma, Z.; Wang, S.; Xu, X.; Xiao, F. A supervisory control strategy for building cooling water systems for practical and real time applications. *Energy Convers. Manag.* **2008**, *49*, 2324–2336. [CrossRef]

34. Shan, K.; Fan, C.; Wang, J. Model predictive control for thermal energy storage assisted large central cooling systems. *Energy* **2019**, *179*, 916–927. [CrossRef]

35. Bianchini, G.; Casini, M.; Pepe, D.; Vicino, A.; Zanvettor, G.G. An integrated model predictive control approach for optimal HVAC and energy storage operation in large-scale buildings. *Appl. Energy* **2019**, *240*, 327–340. [CrossRef]

36. Ahmad, T.; Chen, H. Short and Medium-term Forecasting of Cooling and Heating load demand in Building Environment with Data-Mining based Approaches. *Energy Build.* **2018**, *166*, 460–476. [CrossRef]

37. Horowitz, S.; Mauch, B.; Sowell, F. Forecasting residential air conditioning loads. *Appl. Energy* **2014**, *132*, 47–55. [CrossRef]

38. Wang, H.; Wang, H.; Zhou, H.; Zhu, T. Modeling and optimization for hydraulic performance design in multisource district heating with fluctuating renewables. *Energy Convers. Manag.* **2018**, *156*, 113–129. [CrossRef]

39. Valiantzas, J.D. Explicit power formula for the Darcy-Weisbach pipe flow equation: Application in optimal pipeline design. *J. Irrig. Drain. Eng. Asce* **2008**, *134*, 454–461.

40. Shaikh, M.M.; Massan, S.H.; Wagan, A.I. A new explicit approximation to Colebrook's friction factor in rough pipes under highly turbulent cases. *Int. J. Heat Mass Transf.* **2015**, *88*, 538–543. [CrossRef]